J Mater Sci (2022) 57:16258–16279

Chemical routes to materials

Polymer-bonded CdTe quantum dot-nitroxide radical nanoprobes for fluorescent sensors

Merve Karabiyik[1] and Özgenç Ebil[1,*]

[1] *Department of Chemical Engineering, Izmir Institute of Technology, Urla, Izmir 35430, Turkey*

Received: 6 May 2022
Accepted: 15 August 2022
Published online: 26 August 2022

ABSTRACT

A novel functional polymer-bonded quantum dots (QDs)-nitroxide radical complex was demonstrated. In the first part of the study, the synthesis of polymer thin films via initiated chemical vapor deposition (iCVD), functionalization of polymer thin films with amine functional groups, and attachment of QDs to polymer surface were demonstrated. Fourier transform infrared spectroscopy and energy-dispersive X-ray spectroscopy together with fluorescence spectroscopy studies revealed that aliphatic primary amine (propylamine) was very effective for the functionalization of iCVD deposited poly(glycidyl methacrylate) (pGMA) and its copolymer with diethylaminoethyl methacrylate (p(GMA-co-DEAEMA)) and also QD attachment to functionalized polymer surface. In the second part of the study, the synthesis and attachment of Quantum Dot-4Amino TEMPO (QD-4AT) nanoprobes to functionalized pGMA thin films and feasibility of using them as fluorescent sensor structures were investigated. It was found that high initial 4AT concentration and long (24 h) interaction times are beneficial for nanoprobe synthesis. Electron paramagnetic resonance (EPR) spectroscopy analysis revealed the existence of covalent bond between QD and 4AT when 1-ethyl-3-(3-dimethylaminopropyl) carbodiimide was used during synthesis. EPR analysis together with fluorescence microscopy investigation confirmed the successful attachment of nanoprobes to polymer surface. Time-depended fluorescence quenching analysis revealed that more than 50% reduction in fluorescence intensity within 15 min demonstrating the potential of polymer bonded QD-4AT nanoprobes in various sensor applications.

Handling Editor: Maude Jimenez.

Address correspondence to E-mail: ozgencebil@iyte.edu.tr
E-mail Address: merveozpirin@iyte.edu.tr

https://doi.org/10.1007/s10853-022-07640-8

GRAPHICAL ABSTRACT

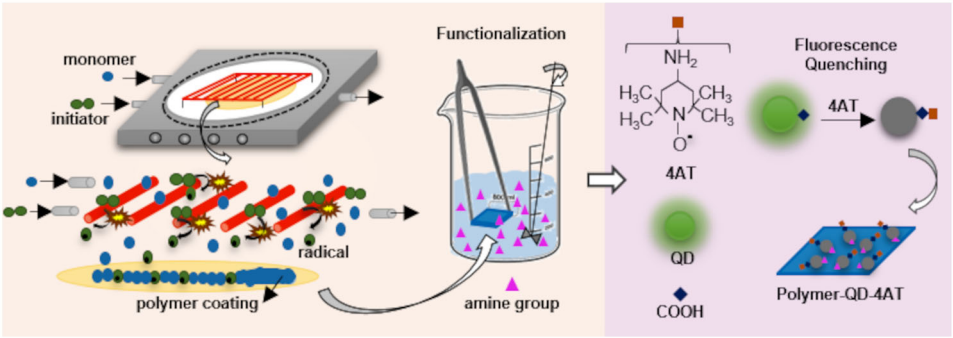

Introduction

Semiconductor nanoparticles, or *quantum dots* (QDs), are of particular interest in biological and chemical sensor applications due to their wide absorption and narrow emission spectra, high quantum efficiency, photo-bleaching resistance, and high photochemical stability compared to other fluorophores [1–7], and they are also increasingly sought after in labeling, imaging and detection applications [8–11]. In recent years, fluorescent sensor studies in which QD nanoparticles were used for different substance detection have attracted much attention [12–17]. Various techniques such as atomic absorption spectrometry, atomic emission spectrometry and inductively coupled plasma mass spectrometry have been used to detect target materials in the chemical or biological fields [18]. Although these conventional techniques have high sensitivity and accuracy, they require complex operators which limit their applications especially in terms of bulky instrumentation, extensive sample preprocessing and in situ analysis [18]. Electrochemical methods, surface plasmon resonance detections, quartz crystal microbalance, chemiluminescence (CL) and fluorescence methods are among the newly developed sensing platforms [19–21]. Among them, fluorescence methods have the advantages of high sensitivity, high accuracy, and relative simplicity [22, 23]. The controlled QD fluorescence quenching (decreasing the fluorescence intensity) phenomenon, which has led to the development of special fluorescent nanoprobes, has been particularly exploited in fluorescent sensor applications [12, 13, 24–26]. In literature studies, the most effective quenchers of fluorescence of organic fluorophore were found to be nitroxide radicals which are also called as profluorescent nitroxides [12, 13, 16, 17]. Fluorophores join a fluorescent moiety labeled with a paramagnetic nitroxide, and in these spin-labeled profluorophores, the paramagnetic nitroxide radical acts as an effective quencher of the fluorophore. As a result, fluorophore-nitroxide complex can be an on–off switch when the paramagnetic nitroxide is transformed to a diamagnetic species such as hydroxylamine or alkoxyamine [12, 13, 25, 27, 28]. There are many studies in the literature based on profluorescent nitroxides, especially nitroxide radical 2,2,6,6-tetramethylpiperidine-N-oxide (TEMPO) for evaluation of quenching effect on the emission of different QDs [12, 14–17, 26, 29]. It was shown that stronger binding can be achieved to the QD surface with functionalized TEMPO radical compared to non-functionalized form of TEMPO [12, 15, 29]. Tansakul et al. [12] studied four different ligand-bearing TEMPO molecules for quenching of QDs and compared the radicals with respect to effectiveness in fluorescence quenching. Quenching efficiency measurements based on the concentration of nitroxide required to achieve a 50% reduction in the emission intensity revealed that 4-Amino TEMPO (4AT) is three times more effective as a quencher than carboxylic acid nitroxide, which is an order of magnitude more effective than amino pyrrolidine

nitroxide and bisamino nitroxide, respectively (4AT > carboxylic acid nitroxide > amino pyrrolidine nitroxide > bisamino nitroxide) [12].

The main purpose of this study is to develop a polymer-bonded QD-4aminoTEMPO nanoprobe as a sensor structure based on the fluorescence quenching. In the literature, similar nanoprobe structures have been demonstrated only in liquid media rendering them single-use, disposable and non-reusable sensors. The synthesis of a polymer-bonded nanoprobe structure, its suitability for use in sensor applications and its fluorescence performance have not been shown in the literature before. It was shown that 4AT, which is also used as quencher in this study, is the most effective quencher in the fluorescence quenching of the QDs [12]. Figure 1 shows non-functionalized TEMPO radical and 4 different ligand-bearing TEMPO radicals.

CdSe and CdTe QDs are the most preferred quantum dots in visible light applications, immunolabeling, in vivo imaging, sensor applications, etc. CdSe and CdTe QDs with carboxylic acid capping ligands can be easily attached to amine-functionalized surfaces [6, 7, 30–32]. Combining the unique optical properties of QDs with flexibility of polymers offers great potential especially for sensing applications. In particular, the integration of sensor structures containing QDs into mechanically and chemical durable polymer films would be useful to make them reusable as previously demonstrated the sensor structures are generally disposable and easily degradable in liquid media [33]. A variety of methods have been used in the literature for polymer surface modification and functionalization such as physicochemical methods including thin film coating, bulk phase desorption, etc., and mechanical methods including micromanipulation and roughening. In addition, biological methods, physical adsorption, and chemical conjugation have also been successfully applied for surface modification of polymers [34–39]. Thin-film coating methods attract attention as a versatile and powerful tool for the modification of surfaces due to the ability of immobilization of different surface functionalities on polymer and better binding of the film to the substrate compared to other methods [40]. Thin-film coating methods are generally classified under wet and dry processes. Wet processes have some drawbacks associated with solvent-substrate interaction, uniformity, temperature control, impurities, etc. [41, 42].

In recent years, a novel technology, initiated chemical vapor deposition (iCVD), has become very popular technique for the deposition of variety of polymer films due to its low thermal budget and higher deposition rates [41]. In iCVD method, the unsaturated bonds of the monomer units adsorbed on the substrate surface are activated by free radicals produced during the thermal decomposition of an initiator molecule (typically at low filament temperatures of 200–400 °C) to form monomer radicals on the substrate surface where they polymerize (substrate temperatures of 0–40 °C) [43]. In iCVD process, the free radical polymerization takes place in solid phase without any solvent. Substrates with complex geometries can be coated conformally using iCVD with high uniformity and without any solvent related issues that are seen in wet processes [41, 43, 44]. In addition, low-temperature iCVD process enables coatings on temperature sensitive materials such as paper, polymers, membranes, etc., without damaging functional groups of the monomers with precise thickness and morphology control [41, 43–45]. It has been demonstrated that the functional groups of the monomers are successfully transferred to the polymeric films formed by preserving their properties [41, 43–45]. Different types of surfaces including

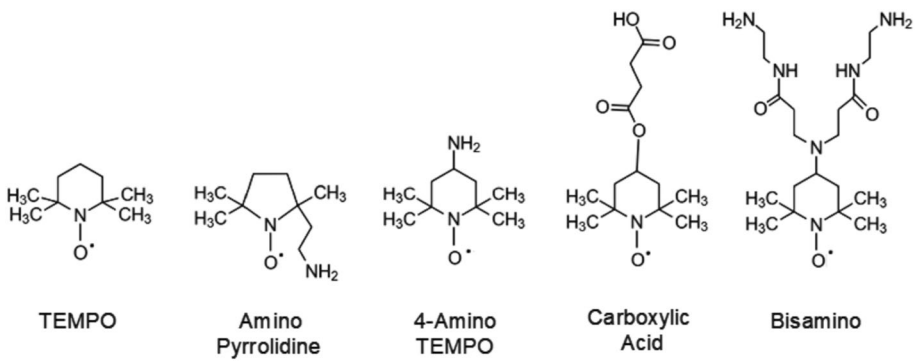

Figure 1 Non-functionalized TEMPO radical and commonly used ligand-bearing nitroxide radicals.

fabric, plastic, silicon, inorganic semiconductor materials, glass, microporous membranes, carbon nanotubes, etc., have been found to be successfully coated via iCVD [46–49]. When compared to other CVD methods such as plasma enhanced chemical vapor deposition (PECVD) and hot wire chemical vapor deposition (HWCVD), iCVD has been the most preferred CVD method for the fabrication of thin polymeric films due to fast deposition rates, low process temperature and acceptable vacuum levels, ability to coat complex 3D geometries conformally, and precise film thickness and microstructure control [50].

Among many other polymeric materials, poly(glycidyl methacrylate) (pGMA), is one of the most suited iCVD polymer due to its epoxy group that can be converted into different kinds of functionalities via ring-opening reactions with several nucleophiles [41–43, 51–55]. Especially, cross-linked (either via ring-opening or copolymerization) pGMA is both mechanically and chemically highly durable in harsh environments making it suitable for protective coating applications. In addition, a variety of chemical groups such as primary amine, sulfhydryl, or hydroxyl groups can be covalently bonded to pGMA (with nucleophilic attack) through the ring-opening reaction leading to further functionalization and modifications of polymeric or inorganic surfaces. The rate of ring-opening reaction varies with the type of nucleophile used [32, 41, 56–64]. In particular, amine functional surfaces have attracted special attention for sensor applications since they react with several groups such as epoxy, aldehyde, carbonyl, carboxylic acid, and sulfonyl chloride [32, 64]. It has been shown that using tertiary amines in epoxy ring opening reactions are preferred since they are considered as highly reactive catalysts for nucleophilic ring-opening reactions under appropriate conditions [1, 41, 65]. Copolymers containing dimethyl amino ethyl methacrylate (DMAEMA), diethyl amino ethyl methacrylate (DEAEMA), diisopropyl amino ethyl methacrylate (DiPAEMA) and morpholinoethyl methacrylate (MEMA) have been found to be highly effective in these reactions [2]. In the literature, epoxy ring opening reaction by DEAEMA that contains tertiary amine group was proven to be very efficient [41, 65]. In addition, several studies were performed by investigating of the role of amine and hydroxyl-containing compounds (water, alcohols, phenols, acids) which considerably promote the interaction of epoxy compounds with amines and other nucleophilic reagents [14]. In the presence of hydroxyl-containing compounds, the epoxy ring carbon atom becomes more sensitive to nucleophilic attack. Ethanol was used in reaction medium to catalyze the epoxy ring opening reaction successfully [60]. However, it is still difficult to conclude whether copolymers containing tertiary amines or homopolymers to catalyze the epoxy ring opening reaction in an alcohol solution is more effective.

In this study, two different methods were used for epoxy ring-opening reaction, one involving DEAEMA with tertiary amine group to catalyze the ring opening reaction of pGMA, and the other in which ethanol was used to catalyze the ring opening reaction of pGMA homopolymer. The aim of the study is to develop robust, polymer-bonded QD nanoprobes as an alternative to the single use and easily degradable sensor structures.

Here, in the first part of the study we report iCVD synthesis and functionalization of pGMA and p(GMA-co-DEAEMA) copolymer thin films via epoxy ring opening reactions to enable the binding of CdTe QDs on the functionalized polymeric surfaces. The effect of different amine functional groups, aromatic primary amine (aniline), aliphatic primary amine (propylamine) and aliphatic tertiary amine (Et_3N) on epoxy ring opening reaction and QD attachment were also evaluated.

In the second part of the study, we report the synthesis and attachment of QD-4AT nanoprobes to functionalized pGMA thin films (selected as the better method for epoxy ring opening) and the feasibility of using QD-4AT nanoprobes as fluorescent sensor structures for sensor applications. The covalent attachment of nanoprobes to polymer surface opens up the possibility of using the sensor multiple times as opposed to solution-based single use fluorescent sensors reported in the literature.

Materials and methods

The study consists of two parts in terms of development of polymeric sensor nanoprobe complex. In the first part, functionalization of iCVD deposited polymers with different amine functional groups by epoxy ring opening reactions to bind CdTe QDs on the functionalized polymers was carried out. The effect of different amine groups on functionalization

was evaluated. In the second part of the study, the interaction between QDs and 4-Amino TEMPO (4AT) was examined by electron paramagnetic resonance spectroscopy (EPR). The effect of reaction time on binding performance and the type of bonding between QDs and 4AT molecules were investigated. In addition, the fluorescence quenching mechanism was investigated by fluorescence analysis and the suitability of QD-4AT complex for fluorescent sensor applications was evaluated by integrating QD-4AT complex to polymer surface.

Homo- and copolymer deposition in iCVD system

A custom-built iCVD system was used to fabricate homo- and copolymer films. The vacuum chamber had a backside cooled via an external circulator enabling a substrate temperature between − 20 and 50 °C with 0.1 °C accuracy. Thermal energy for decomposition of the initiator was supplied by a heated filament array (Nichrome, 80% Ni/20% Cr) placed 3 cm above the cooled substrate. GMA (Sigma-Aldrich, 97%) as epoxy monomer and DEAEMA (Sigma-Aldrich, 99%) as amine group monomer were used without further purification. GMA and DEAEMA monomers were heated to 65 °C and 80 °C, respectively, in stainless steel containers. Tert-butyl peroxide (TBPO, Sigma-Aldrich, 98%) was used as initiator at room temperature. All depositions were performed on crystalline silicon (c-Si) substrates.

Epoxy ring opening reactions

Procedure 1: p(GMA-co-DEAEMA) amine functionalization

Copolymer p(GMA-co-DEAEMA) thin films were fabricated using DEAEMA and GMA monomers via iCVD. As a low-temperature process, iCVD process allows retention of functional groups during polymerization as shown in Fig. 2. Resulting copolymer film contains both the epoxy and the amine group, and surface functionalization can be carried out on copolymer films. Three different amine functional groups were used to compare their reactivity in the epoxy ring opening reaction. 1M aqueous solutions of aromatic primary amine (Aniline, Sigma-Aldrich, 99.5%), aliphatic primary amine (propylamine, Sigma-Aldrich, 98%) and aliphatic tertiary amine (Et_3N, Sigma-Aldrich, 99%) were prepared. iCVD fabricated copolymer films were immersed into mechanically stirred amine solutions at room temperature for two hours. Copolymer films were then rinsed with deionized water and dried at 60 °C for 1 h under vacuum.

The formation of donor–acceptor complex interactions via a polymer with electron donor groups in its

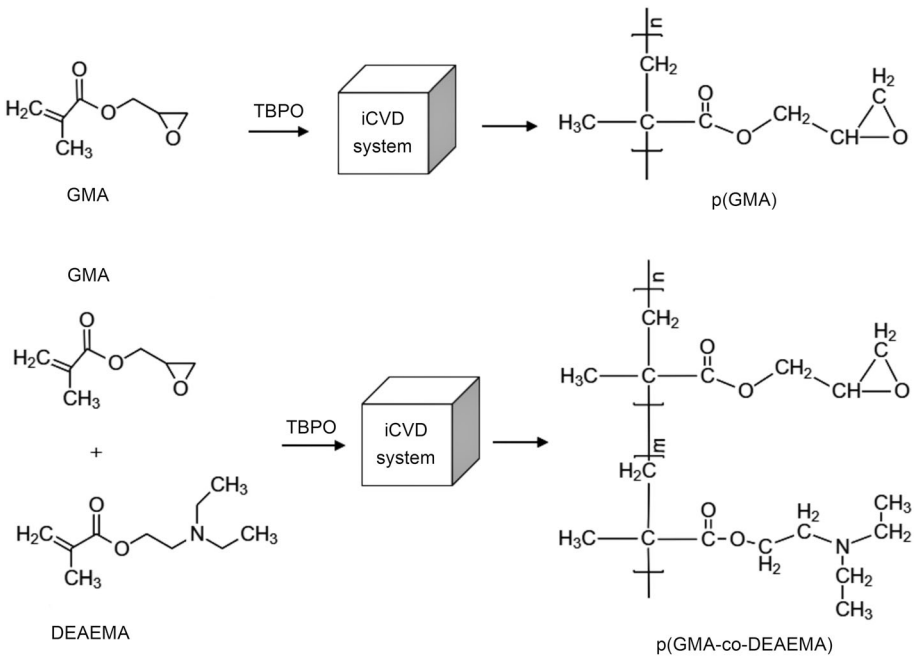

Figure 2 Synthesis of pGMA homopolymer (top) and p(GMA-co-DEAEMA) copolymer (bottom) via iCVD.

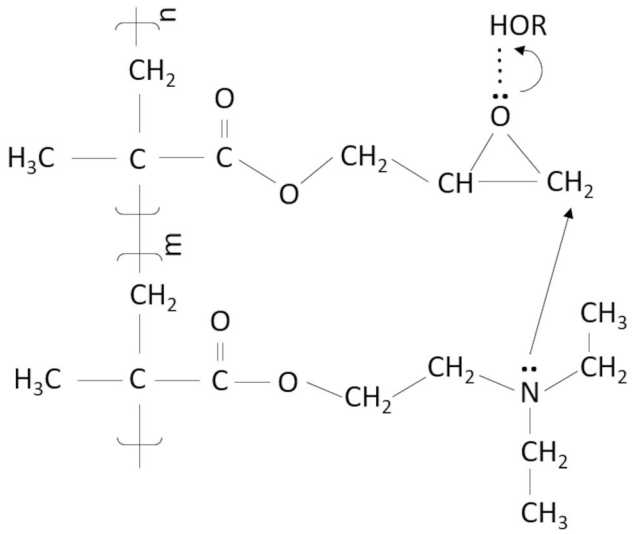

Figure 3 Epoxy ring opening reaction mechanism in p(GMA-co-DEAEMA) copolymer.

structure has a complex mechanism [66]. Donor–acceptor complex interaction between the electron donor groups in the polymer which is tertiary amine group in DEAEMA and acceptor group which is hydroxyl-containing compound (water) enables epoxy ring opening and attachment of amine groups in the environment with the formation of both intramolecular and intermolecular interactions. The general view of the mechanism is given in Fig. 3.

Procedure 2: pGMA homopolymer amine functionalization

Homopolymer pGMA films fabricated via iCVD were functionalized using a slightly different process than copolymer functionalization. Ethanol solution was used as a catalyst for the epoxy ring opening reaction in the absence of DEAEMA monomer. pGMA homopolymer coatings were immersed into 1 M ethanol solutions of aniline, propylamine and Et_3N separately and stirred at 60 °C for 2 h. After ring opening reaction, homopolymer films were rinsed with ethanol and dried at 60 °C for 1 h under vacuum.

During the reaction, donor–acceptor complex interactions occur between the amine and the hydroxyl-containing compound (HOR). The general mechanism of addition of amines to the epoxy ring of pGMA is shown in Fig. 4.

The addition of amines proceeds through a preliminary formation of fairly stable donor–acceptor complexes of the epoxy compound with ethanol, and

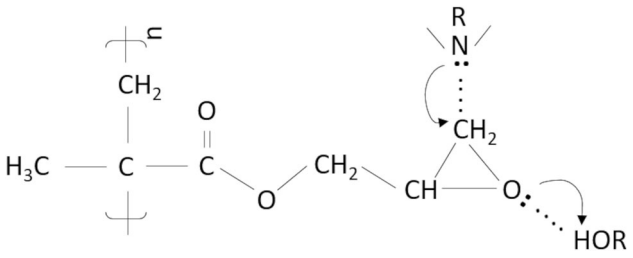

Figure 4 Epoxy ring opening reaction mechanism in pGMA homopolymer.

then with a subsequent nucleophilic attack of the amine on this complex [60, 66]. In this way, the bonding of the amine group to the open epoxy ring takes place. After the amine group is attached to opened epoxy ring, other unbound amine molecules take on the role of forming donor–acceptor complexes with the hydroxyl-containing compound (HOR) to bind to other opened epoxy rings in the polymer film.

QD attachment to functionalized thin films

There are many studies in the literature reporting the binding of QDs to the polymer surface via the amine groups. Binding of QDs to the polymer surface generally occurs as a result of amide bond formation between the -COOH group of QDs and the amine groups on the polymer surface [32, 67–69]. It is generally preferred that carbodiimide compound should be present in the reaction medium because it enables QD activation [32, 69]. The most commonly used carbodiimide compounds in literature are N, N′-dicyclohexylcarbodiimide (DCC) [32, 67] and N-(3-dimethylaminopropyl)-N′-ethylcarbodiimide (EDC) [68, 69].

In the first part of this study, DCC was used to activate QDs in order to bind them on polymer surface by amine groups with formation of amide bond. One milligram of carboxylic acid functionalized CdTe QD (Sigma Aldrich, λ_{em} = 520 nm) was dispersed in 20 ml deionized water and was ultrasonicated for 30 min to obtain a uniform dispersion. A small amount of DCC (Sigma Aldrich, ≥ 99.0%) (< 1 mg) was added to the dispersion. Functionalized homo- and copolymers were immersed into QD dispersion at 60 °C for 2 h. The films then were rinsed with deionized water to remove unbound QDs from the surface and dried at 60 °C for 1 h under vacuum. 60 °C was used instead of room temperature to

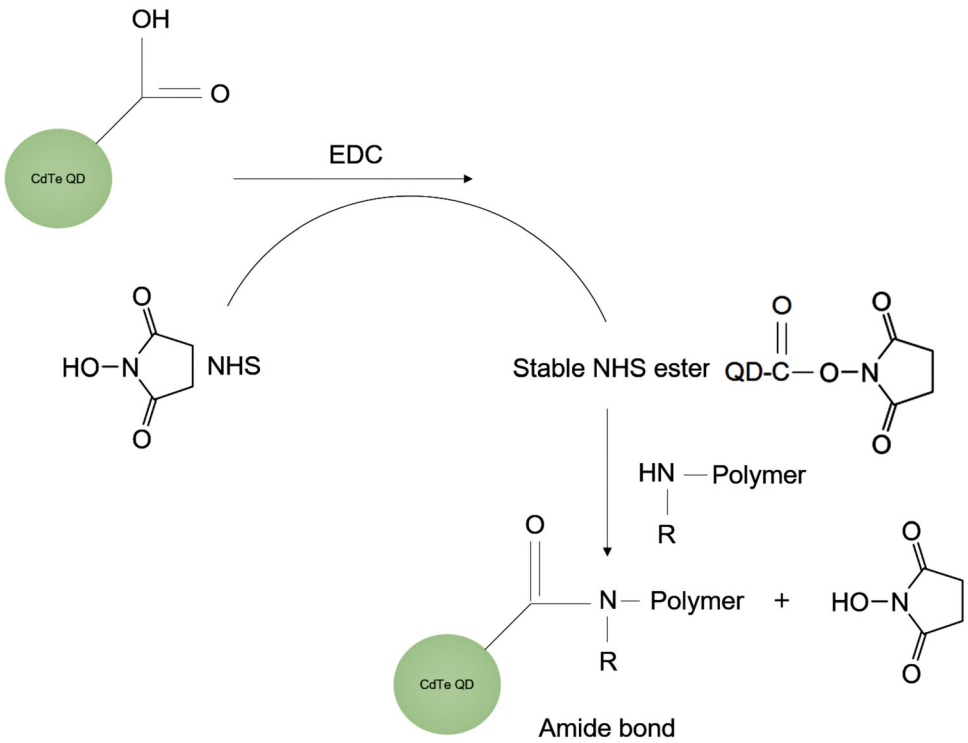

Figure 5 Carbodiimide-based coupling reaction. The –COOH groups on the QD surface are activated by EDC and addition of NHS yields a stable reactive NHS ester intermediate that reacts with NH groups on the polymer film to yield a stable amide bond.

enhance DCC solubility in water. However, in the literature studies, it was observed that the same process could also be performed using EDC at room temperature [67, 68]. Due to lower reaction temperature, EDC/N-hydroxysuccinimide (NHS) was used in the binding of QD to the polymer surface in the second part of the study which is related with QD-4AT nanoprobe integration on polymer surface by interaction of QDs and amine groups of polymer. The bonding mechanism between QD and amine group of polymer is shown in Fig. 5. Amide bond formation can be performed successfully with the presence of EDC and NHS in reaction medium. As a result, –NH groups along the polymer chain can easily react with –COOH functionalized QDs through EDC/NHS chemistry.

Preparation of CdTe QD-4AT nanoprobe

CdTe QD-4AT nanoprobe was synthesized by binding 4-Amino TEMPO (4AT) molecules (as shown in Fig. 1) to CdTe QDs. Two procedures with different QD activation and binding process times were followed to investigate the effect of QDs and 4AT interaction time on binding to the QD surface. All other conditions were kept the same. CdTe QD dispersion was prepared using deionized water with ultrasonication for 30 min at 25 °C. A solution containing excess amount of EDC and NHS was prepared with phosphate buffered saline (PBS) (10 mM and pH: 7.4) and added to QDs dispersion to activate -COOH groups on QDs in PBS buffer (pH: 7.4). Continuous gentle stirring was applied to the mixture for 30 min (for procedure A) and 2 h (for procedure B) at 25 °C. Next, 4AT solution was prepared using PBS buffer (pH: 7.4) and then added to activated QDs mixture. Continuous gentle stirring for 4 h (for procedure A) and for ~ 24 h (for procedure B) at 25 °C was applied. Figure 6 describes the preparation of -COOH functionalized CdTe QD-4AT nanoprobe. Figure 7 shows experimental steps for CdTe QD-4AT complex preparation procedure and EPR analysis of the complex.

Attachment of QD-4AT nanoprobes to polymer surface

To attach QD-4AT nanoprobes to the surface of iCVD polymers, thin-film polymer was immersed into the solution for 2 h, while QD-4AT nanoprobe formation procedure, as shown in Fig. 7a, was being carried out. In addition, a reference solution was also prepared containing only 4AT without QDs by using the same procedure and iCVD polymers were dipped

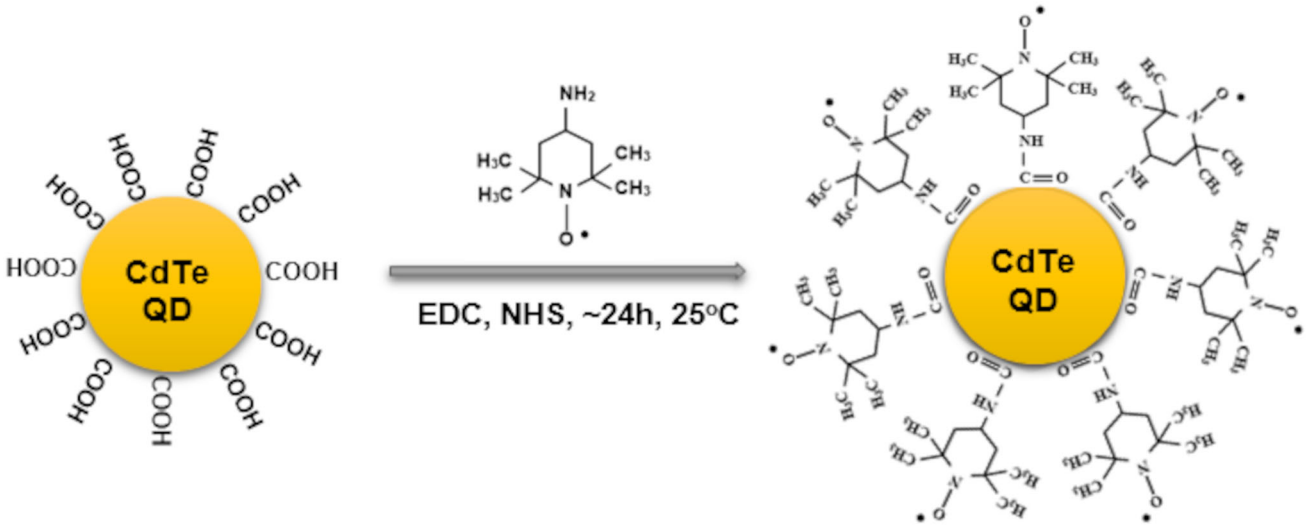

Figure 6 COOH functionalized CdTe QD-4AT nanoprobe.

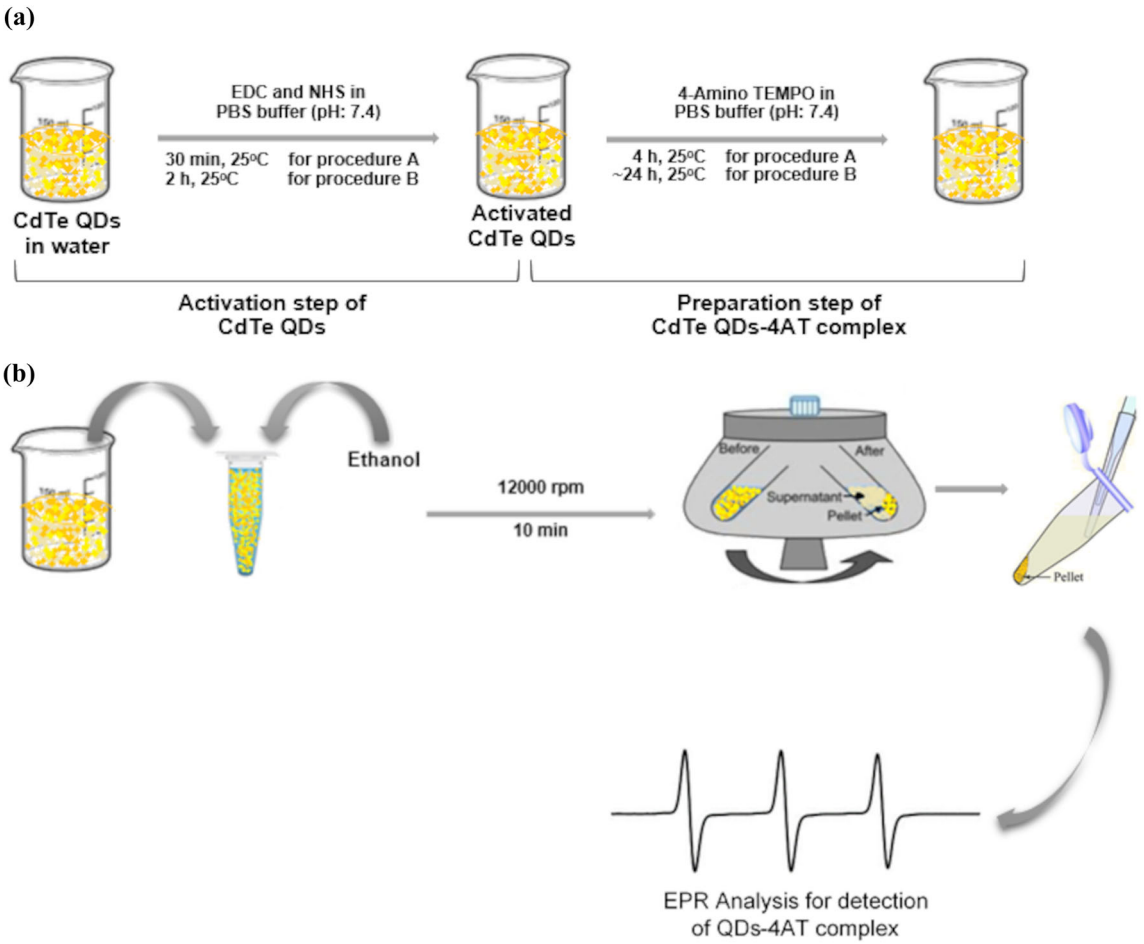

Figure 7 **a** CdTe QD-4AT complex preparation procedure and **b** EPR analysis for the detection of QD-4AT complex.

into this reference solution for comparison. EPR spectroscopy was used to confirm binding of QDs to the polymer surface.

Characterization

Thickness measurements of iCVD polymer films were performed using a Mprobe-Vis20 reflectometer with a spectral range between 400 and 1100 nm. FTIR analysis was used to investigate chemical composition and quality of polymer films. FTIR spectra of samples were taken using a PerkinElmer-UATR Two Spectrometer between 450 and 4000 cm^{-1} with 4 cm^{-1} resolution. In addition to FTIR analysis, energy-dispersive X-ray spectroscopy (EDX) (FEI QUANTA 250 FEG:EDX) was used to investigate chemical composition of the polymer films before and after epoxy ring opening reactions. Water contact angle (WCA) measurements were performed using a Theta Optical Tensiometer. Static contact angle measurements were performed for 1 min by dropping 5 µl water on sample surface. To examine QD and 4AT nitroxide radical interaction both in solution and on the polymer surface, electron paramagnetic resonance spectroscopy (EPR) analysis was performed using a CMS 8400 EPR Spectrometer. Fluorescence spectroscopy (Zeiss-Observer Z1 fluorescence microscope and PerkinElmer LS 55) was used to confirm the attachment of quantum dots onto the film surface and for fluorescence quenching measurements. Excitation and emission wavelength ranges of 300–350 nm and 500–550 nm, respectively, were used for CdTe QDs.

Results and discussion

Polymer synthesis and amine functionalization

In order to find optimum process conditions, initial experiments were carried out for homopolymers by varying monomer/initiator flow rate ratio, reactor pressure, filament and substrate temperatures. Similarly, copolymer films with various composition were fabricated using different monomer flow rates (F_{DEAEMA}:F_{GMA} ranging from 0.12 to 1), reactor pressures and substrate temperatures. Table 1 shows optimized iCVD process conditions, thicknesses and deposition rates for pGMA and pDEAEMA homopolymers, and p(GMA-co-DEAEMA) copolymer used in this study. For all depositions, substrate temperature, T_s, and reactor pressure, P, were kept constant at 35 °C and 250 mTorr, respectively. Resulting film deposition rates varied between 10 and 13 nm/min.

FTIR analysis is a useful tool for evaluation of the quality and chemical composition of polymer films and also confirming complete polymerization that is no monomer is present on the surface of the substrate after deposition in iCVD. FTIR spectra of iCVD deposited pGMA, pDEAEMA homopolymers and p(GMA-co-DEAEMA) copolymer films are given in Fig. 8.

The characteristic absorbance peaks that belong to methacrylates are clearly observed in FTIR spectra of all samples [41, 65, 70–75]. Prominent characteristic peaks between 3000 and 2800 cm^{-1} are assigned to C-H symmetry and asymmetry stretching caused by CH_3 and CH_2 groups; the peak at 1730 cm^{-1} is related to carbonyl group (C=O) stretching vibration. Peaks related to C=C bonds belonging to monomers, like significant peak is at 1640 cm^{-1}, are not observed in iCVD deposited polymers' spectra indicating

Table 1 iCVD process conditions for pGMA and pDEAEMA homopolymers, and p(GMA-co-DEAEMA) copolymer thin films

Process conditions	pGMA	pDEAEMA	p(GMA-co-DEAEMA)
F_{GMA} (sccm)	1.5	–	1
F_{DEAEMA} (sccm)	–	1.2	0.5
F_{TBPO} (sccm)	1	0.8	0.65
T_f (°C)	330	300	300
T_{sub}(°C)	35	35	35
P_{dep} (mTorr)	250	250	250
Thickness (nm)	378 ± 4	312 ± 1	390 ± 4

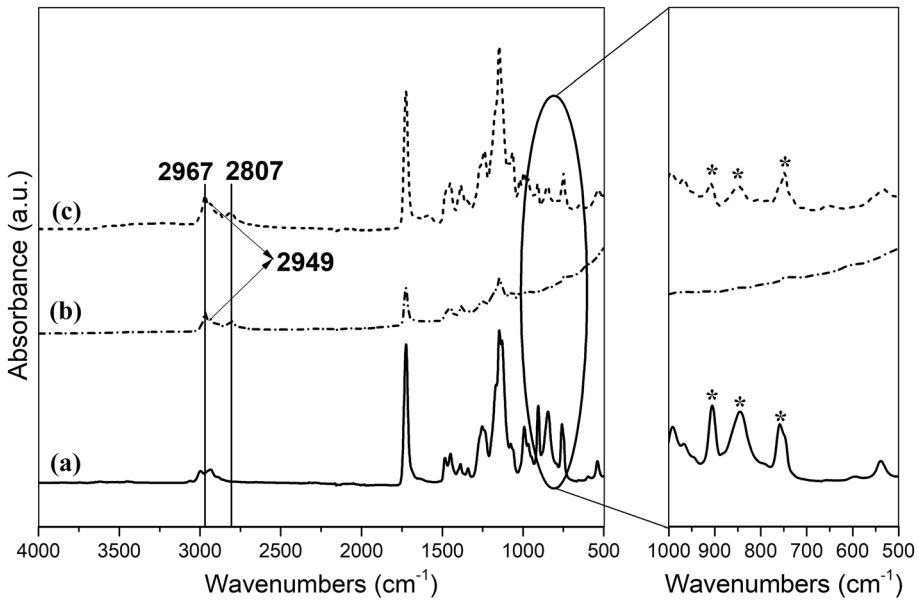

Figure 8 FTIR spectra of **a** pGMA, **b** pDEAEMA, **c** p(GMA-co-DEAEMA) thin films. (*) represent epoxy group peaks.

Table 2 EDX analysis of iCVD deposited pGMA, pDEAEMA homopolymers and p(GMA-co-DEAEMA) copolymer films

Element	pGMA		pDEAEMA		p(GMA-co-DEAEMA)	
	Wt%	Atomic %	Wt%	Atomic %	Wt%	Atomic %
C	60.0	66.7	62.2	67.7	51.8	58.7
O	40.0	33.3	26.2	21.4	46.0	39.1
N			11.6	10.9	2.2	2.2
Total	100.0	100.0	100.0	100.0	100.0	100.0

complete consumption of adsorbed monomers [41, 72, 73]. The characteristic peaks at 906, 846 and 760 cm^{-1} which are belong to epoxy group stretching, are clearly seen in pGMA FTIR spectrum [71, 72, 74, 75]. The peaks at 2967, 2949 and 2807 cm^{-1} are attributed to different C-H vibrations, and $-N(C_2H_5)_2$ functional group [41, 65, 73]. The characteristic peaks of both epoxy and tertiary amine groups are observed in copolymer spectrum confirming successful deposition of p(GMA-co-DEAEMA).

In addition to FTIR analysis, chemical composition of iCVD fabricated films was also investigated before and after epoxy ring opening reactions via EDX analysis. Table 2 shows elemental composition of as deposited iCVD polymer films.

EDX analysis can detect elements with concentrations between 1 and 10 wt% but cannot be used for detection of trace elements. Therefore, it is a useful tool for quick elemental analysis of polymer films before and after ring opening reactions but not for detection of CdTe QDs. For EDX analysis, the signal coming from c-Si substrate was removed and the composition was calculated based on carbon, nitrogen and oxygen elements. In Table 2, the presence of amine groups belonging to DEAEMA in copolymer films was confirmed via EDX analysis.

Table 3 shows elemental composition of pGMA and p(GMA-co-DEAEMA) films after ring opening reactions with aniline, propylamine and Et_3N. The highest nitrogen content was found in propylamine-functionalized copolymers (12.10%) when compared with aniline (6.12%) and Et_3N (4.20%) functionalized copolymers. Similarly, propylamine-functionalized pGMA homopolymer showed higher nitrogen concentration (9.08%) than aniline (6.25%) and Et_3N (2.60%) functionalized pGMA.

According to the EDX results, propylamine reactivity in the epoxy ring opening reaction is higher than aniline and Et_3N. For p(GMA-co-DEAEMA),

Table 3 EDX analysis after p(GMA-co-DEAEMA) copolymer and pGMA homopolymer functionalization with aniline, propylamine and Et_3N

Element	Aniline		Propylamine		Et_3N	
	Wt %	Atomic %	Wt %	Atomic %	Wt %	Atomic %
	p(GMA-co-DEAEMA) functionalization					
C	53.2	59.8	50.6	56.9	65.8	71.6
O	40.4	34.1	36.8	31.0	29.7	24.2
N	6.4	6.1	12.6	12.1	4.5	4.2
Total	100.0	100.0	100.0	100.0	100.0	100.0
	pGMA functionalization					
C	54.0	60.5	52.8	59.1	54.0	60.8
O	39.5	33.2	37.8	31.8	43.3	36.6
N	6.5	6.3	9.4	9.1	2.7	2.6
Total	100.0	100.0	100.0	100.0	100.0	100.0

amine containing DEAEMA monomer and for pGMA, ethanol act as catalyst during epoxy ring opening reaction. As expected, the reactions were successfully catalyzed by both routes [2, 41].

The purpose of using amine groups in this study is to ensure bonding of QD nanoparticles onto pGMA polymer via epoxy ring opening reaction. CdTe QDs can be attached to polymer surface over amine groups via formation of bond between amine groups and QDs' -COOH groups [32, 41]. WCA measurements were performed to investigate whether the polymer surfaces are successfully functionalized with amine groups in the epoxy ring opening reaction and to confirm the previous EDX and FTIR analysis results. It is well known that both pGMA and pDEAEMA homopolymers are hydrophilic in nature [41, 60]. For this purpose, in the analysis, the change in hydrophilicity of polymer surfaces after ring opening reactions with different amine groups was examined. WCA values and changes in the water droplets after 1 min are shown in Fig. 9.

WCAs of iCVD deposited pGMA and pDEAEMA homopolymers were measured as $71.6 \pm 4°$ and $81.7 \pm 1°$, respectively. These results are in good agreement with studies in the literature as pGMA is more hydrophilic than amine group polymers [41, 60]. As expected, p(GMA-co-DEAEMA) copolymer was found to have a WCA of $77.1 \pm 0.7°$. WCA measurements of pGMA homopolymer and p(GMA-co-DEAEMA) copolymer were also taken after epoxy ring opening reactions. Homo- and copolymer films exhibited different WCAs depending on the presence of functional groups. For ring opening reactions, very reactive primary aliphatic amine (propylamine) and tertiary aliphatic amine (triethylamine (Et_3N)), and

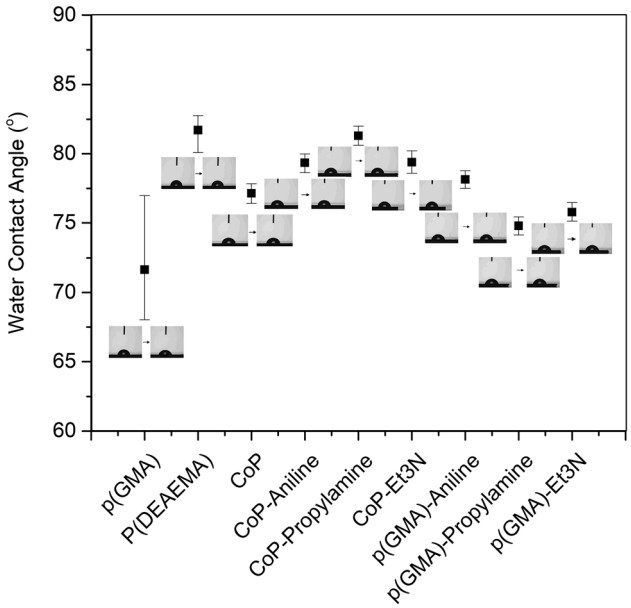

Figure 9 Water contact angle measurements for pGMA, pDEAEMA, their copolymer (CoP), functionalized CoP and pGMA after epoxy ring opening reaction with aniline, propylamine and Et_3N, respectively.

less reactive primary aromatic amine (aniline) were used. It was observed that ring opening reaction with amines reduces hydrophilicity of pGMA and p(GMA-co-DEAEMA) copolymer films. This was expected since amine functional groups are low surface energy components [41, 76, 77]. For p(GMA-co-DEAEMA) copolymer, the highest WCA was obtained with propylamine reaction. Triethylamine and aniline resulted in slightly lower WCAs. For pGMA homopolymers, the highest WCA was observed with aniline. Slightly lower WCAs with aliphatic amine group sources, propylamine and

Et_3N were observed. Similar to aromatic amines, aliphatic amines directly bond to epoxy ring, but the presence of unreacted amine tail ends in the aliphatic amines increases surface wettability. Therefore, lower WCAs were observed with propylamine and Et_3N compared to aniline in pGMA homopolymer [76–78].

However, this behavior was not observed in p(GMA-co-DEAEMA) copolymers. To examine whether the amine groups maintain their reactivity and to evaluate the effectiveness of CdTe QD attachment procedure, fluorescence microscopy analysis was performed as shown in Fig. 10.

Linearly stretched fluorescence microscopy images showed relatively uniform emission over the entire sample surface for both pGMA homopolymer and p(GMA-co-DEAEMA) copolymers regardless of the amine groups used. The bright spots that exist in images are either CdTe QD agglomerates or impurities that scatter the emission from QDs. Some of these bright spots are distributed randomly over large areas, but most of them are concentrated on or near surface defects such as cracks on the film surface or physical damage seen in Fig. 10b due to mishandling of the samples and around surface impurities (dust and other particles) as seen in Fig. 10c and d. However, fluorescence microscopy images are still useful to evaluate the effectiveness of QD attachment procedure and reveal that QD attachment was performed successfully for both homo- and copolymer films.

Considering the EDX, WCA and fluorescence microscopy analysis results, it is reasonable to state that epoxy ring opening routes where ethanol was used as catalyst for homopolymer and DEAEMA monomer was used as catalyst for copolymer coating are successful and QD attachment procedure was effective for both homo and copolymer films. The results obtained in the first part of this study are consistent with literature studies. It was reported that aliphatic primary or secondary amines can catalyze ring opening reactions of epoxides successfully while primary and secondary aromatic amines are not capable of catalyzing epoxide polymerization. The studies also indicated that tertiary amines can be used by themselves as catalysts of epoxide polymerizations and curing agents [79]. Besides, tertiary amine containing copolymer coatings increase the reactivity of the epoxide reactions when compared with amine-free coatings. It was also reported that the presence of alcohols also leads to high reaction rates in polymerization of epoxides [41, 65, 79].

Characterizations of QD-4AT nanoprobe

In the second part of the study, the synthesis of QD-4AT nanoprobe, its attachment to functionalized polymer thin films and evaluation of the feasibility of

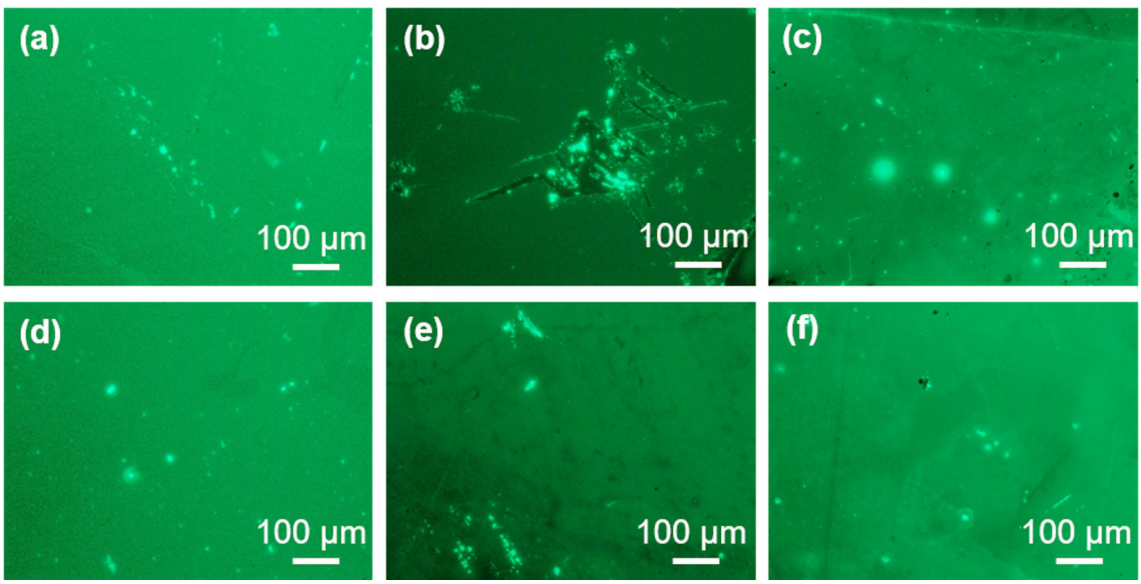

Figure 10 Fluorescence microscopy images of CdTe QD attached surfaces of (**a–c**) aniline, propylamine and Et_3N functionalized p(GMA-co-DEAEMA), and (**d–f**) aniline, propylamine and Et_3N functionalized pGMA, respectively. Excitation and emission wavelength ranges were 300–350 nm and 500–550 nm, respectively.

polymer-bonded QD-4AT nanoprobe as fluorescent sensor structure were investigated using pGMA homopolymer. The nanoprobe was synthesized either by the formation of a covalent or weak bond between QD and 4AT. QD-4AT nanoprobe complex before and after binding to iCVD deposited pGMA films was characterized via EPR analysis to investigate the bonding of nanoprobes to the polymer surface by comparing the EPR data.

The effect of QD and 4AT interaction time was examined by comparing EPR spectrum of the reference study and EPR spectra after procedures A and B which have 4- and 24-h interaction times, respectively. In addition, the effect of initial 4AT concentration on QD-4AT complex formation was investigated. The effect of QD and 4AT interaction time was evaluated based on the change in the amount of bound nitroxide to CdTe QDs for procedures A and B with comparison to free 4AT as shown in EPR spectra of samples in Fig. 11.

In Fig. 11, EPR spectra of free 4AT reference study illustrates the three characteristic ^{14}N hyperfine splitting as black line, which is consistent with previously reported studies in literature [12, 16, 29]. In both procedures A and B, the same amount of CdTe QDs was added to 4AT solution. In literature studies, it has been observed that the ratio [4AT]/([4AT] + [QD]) affects line broadening. With a ratio greater than 0.5, sharp peaks are observed as in free 4AT, no line broadening [29]. In this study, [4AT]/([4AT] + [QD]) ratio is greater than 0.9, since the 4AT concentration was much higher than the concentration of CdTe QD. As expected, line broadening was not observed in either procedure as seen in Fig. 11a. However, peak intensities in procedure B were higher when compared with procedure A. Although the same amounts of QD and 4AT were used in both procedures, the interaction of the QD-4AT nanoprobe increased as time increased, which allowed more nitroxide radicals to attach to the QD surface in procedure B. As the amount of 4AT interacting with QD increased, the amount of 4AT detected by EPR also increased. Also, the peak-to-peak height at the high-field peak in EPR signal is slightly less than those at central and low fields for both procedures (Fig. 11b and c). The distortion of high field peak occurs as a result of the interaction between QD and 4AT proving that the nitroxide radical is bound to QD surface [26]. The attachment of 4AT to QD surface causes a slowdown in rotational motion of spin labels. The motion of a nitroxide side-chain is characterized by the effective correlation time, τ_R [26, 80, 81]. In EPR, the molecular freedom of movement is quantitatively related to the rotational correlation time of the nitroxide spin-labeled molecule, and the rotational correlation time is described as [26];

$$\tau_R = 6.51x10^{-10}x\Delta H(0)\left[\sqrt{\frac{h(0)}{h(-1)}} + \sqrt{\frac{h(0)}{h(1)}} - 2\right] \quad (1)$$

where ΔH(0) is the peak-to-peak line width of the mid-field line and the peak-to-peak amplitude of the lateral lines of the peaks from low field to high field

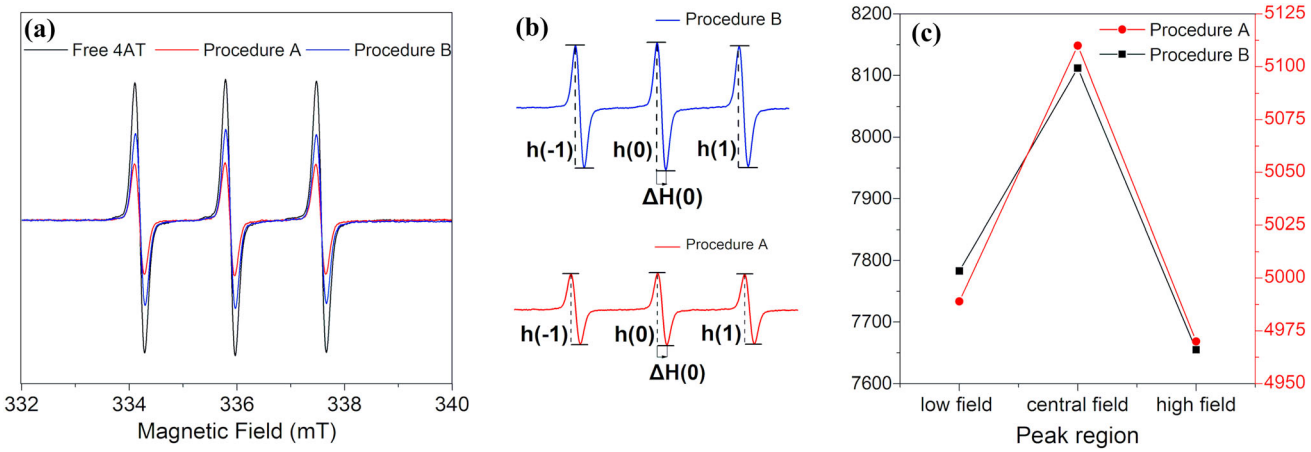

Figure 11 **a** EPR spectra of procedure A (4 h interaction of QDs and 4AT), procedure B (24 h interaction of QDs and 4AT), and free 4AT, **b** parameters (h(-1); h(0); h(1); ΔH(0)) of an EPR spectrum necessary to calculate the effective rotational correlation time (τR), **c** peak to peak height changes for both procedure A and B.

are referred to as h(-1), h(0) and h(1), respectively (Fig. 11b).

Accordingly, the rotational correlation time can be useful to evaluate in which procedure more nitroxide radicals are attached to QD surface. The larger rotational correlation time indicates a slower motional regime after the attachment [26, 80, 81]. The rotational correlation time, τ_R, for procedures A and B was found as 3.018×10^{-12} s and 5.914×10^{-12} s, respectively; therefore, more nitroxide radicals were bound to QD surface in procedure B. Based on this result, procedure B with longer interaction time was selected as main QD-4AT nanoprobe complex formation procedure for the rest of the study.

The effect of initial radical concentration on the formation of QD-4AT complex was evaluated following procedure B. The concentration of 4AT was increased 10 × and 50 × compared to the CdTe QDs concentration in the solution, and EPR analysis was performed as shown in Fig. 12.

As expected, EPR peak intensities of QD-4AT complex are lower than peak intensity of free 4AT due to bonding on QD surface as seen in Fig. 12. Increasing the concentration of 4AT from 10 × to 50 × resulted in an increase in the EPR peak intensity due to higher amount of 4AT molecules which are bonded to QDs. Similar to time studies described in Fig. 11, 4AT concentration was much higher than

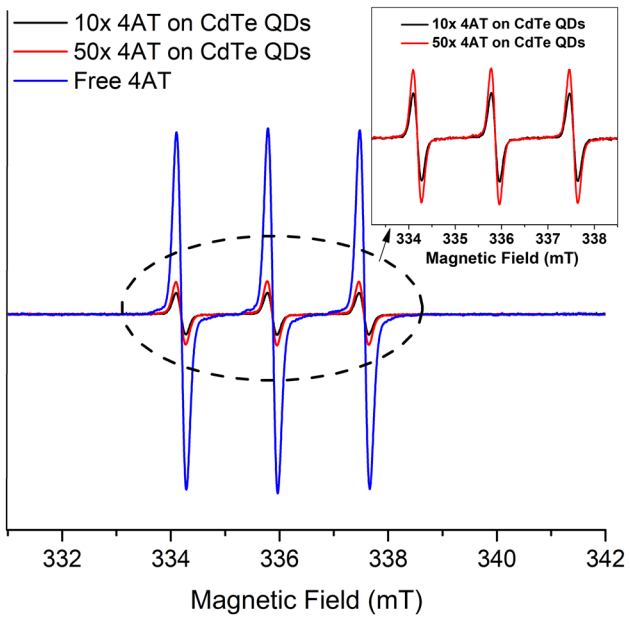

Figure 12 EPR spectra of 4AT at 10 × and 50 × concentration compared with CdTe QDs.

that of CdTe QD. For 10 × and 50 × of 4AT concentrations used, [4AT]/([4AT] + [QD]) ratios were 0.91 and 0.98, respectively; therefore, no significant peak broadening was observed with the formation of QD-4AT nanoprobe complex [29].

To examine whether a covalent or weak bond interaction occurs between 4AT and QD, QD-4AT nanoprobe synthesis procedure was carried out with and without EDC. EPR spectra obtained from the pellet and supernatant samples after centrifugation are given in Fig. 13.

As seen in EPR spectra from pellet samples (Fig. 13a), EPR signals of QD-4AT with EDC are easily identified with three characteristic ^{14}N hyperfine splitting peaks when compared with QD-4AT without EDC. This is a clear validation of formation of QD-4AT complex by covalent bonding of nitroxides to the QD surface activated with EDC. EPR spectra shown in Fig. 13b belong to the supernatant samples of EDC and EDC-free experiments, respectively. Similar to pellet samples, peak intensities are much higher for samples with EDC; however, samples without EDC also show three characteristic peaks with much lower intensities. Therefore, it is reasonable to assume that when EDC was added to the solution, QD activation and the formation of QD-4AT complex occurred with a covalent bond. Without EDC, free TEMPO radicals were not seen in the supernatant medium because EPR intensities were very low, so complex formation may have also occurred with weak bond interaction between QDs and 4AT.

Also, the EPR signals of EDC-free experiment of the supernatant samples were obtained lower than expected when compared with the results of the pellet samples. This may be due to electrostatic bonds. Because electrostatic bonds are more flexible than covalent bonds, 4AT radicals may come closer to the QD surface with electrostatic bonds compared to covalent bonds [12, 15, 26, 29]. It is expected that the EPR signal intensity should be high if covalent bonds are formed between QD and 4AT due to the certain distance between the ligaments, and lower EPR signal should be obtained with weak bonds since the proximity between the QD and 4AT increases due to flexibility in the weak bonds. Based on these results, it can be stated that the formation of QD-4AT complex by weak bonds in the experiments without EDC and existence of covalent bond with the use of EDC were observed in this study.

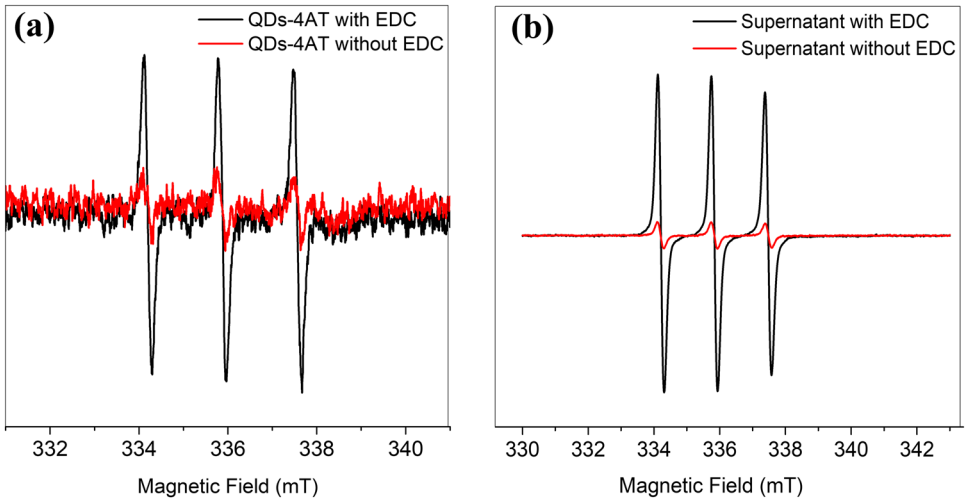

Figure 13 EPR spectra of **a** pellet samples and **b** supernatant samples with and without EDC.

In addition to the interactions between QD and 4AT in the liquid phase, fluorescence quenching was investigated by attaching QD-4AT complex into pGMA homopolymer thin film for fluorescent sensor operation.

Attachment of QD-4AT nanoprobes to pGMA homopolymer

Polymer-QD-4AT nanoprobe complex generation procedure was performed following the procedure described in previous section. EPR spectra of pGMA thin-film coatings immersed in reference solution containing only 4AT molecule and QD-4AT nanoprobe solution are given in Fig. 14.

EPR spectra of pGMA homopolymer coatings given above illustrate that in the absence of QDs, 4ATs could not bind to polymer surface on their own as indicated with a very weak spectrum (black line), as expected. However, when QDs are introduced to 4AT solution for the formation of nanoprobe complex, QD-4AT complex attached to polymer as indicated by the three characteristic ^{14}N hyperfine splitting peaks in EPR spectrum (red line) in Fig. 14.

In order to examine the variation of the spectrum after nanoprobe bonding to the polymer surface, a comparison was made between spectra of 4AT in water and pGMA homopolymer coating after immersed into the QD-4AT complex. EPR spectra were normalized, and then, difference between the signals was examined (Fig. 15).

As seen in Fig. 15, EPR spectra of 4AT in water (blue line) exhibit three very sharp ^{14}N hyperfine splitting peaks. EPR spectrum of pGMA polymer in

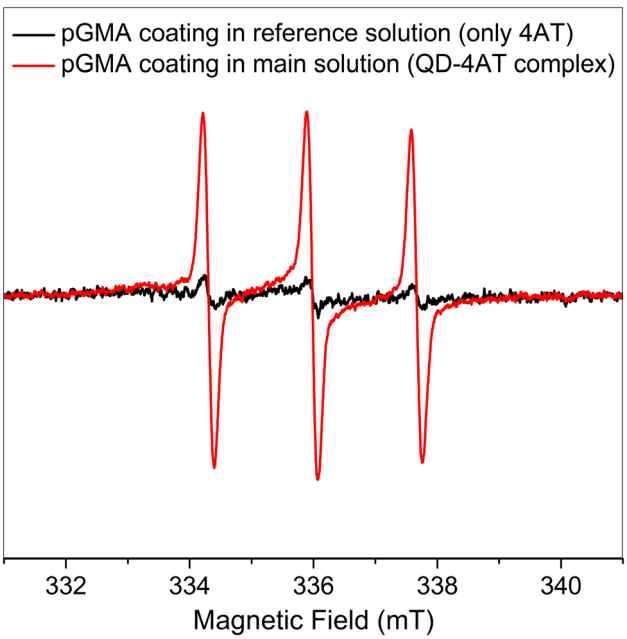

Figure 14 EPR spectra of pGMA homopolymer thin films processed with only 4AT and QD-4AT nanoprobe solutions.

QD-4AT solution (black line) also shows these three peaks, but a significant broadening at peak bases is observed. The peak broadening is a result of restricted motion of the spin labels [82, 83] indicating that QD-4AT nanoprobe is bound to polymer surface. However, clearly identified three distinct and sharp peaks of pGMA polymer in QD-4AT solution also indicate that the radicals are not very close to each other on the polymer surface since more densely packing on the polymer surface would result in very broad peaks. Since the pGMA polymer samples were thoroughly dried, it is not possible to relate sharp

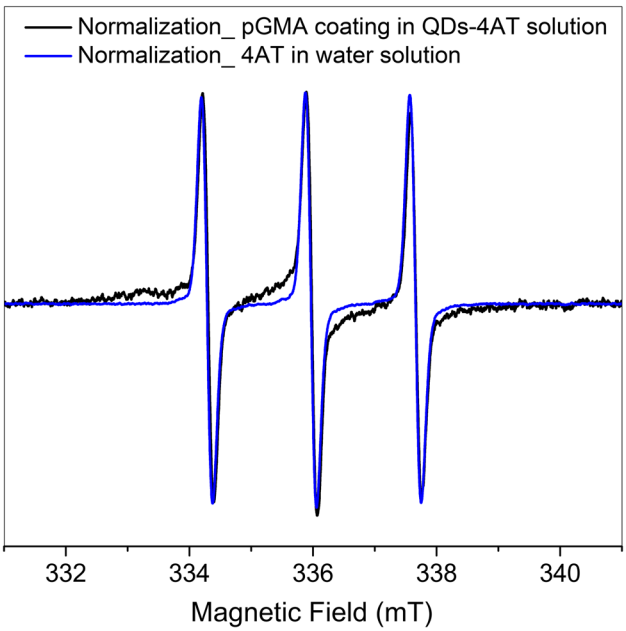

Figure 15 Normalized EPR spectra of pGMA homopolymer thin film in QD-4AT solution and 4AT in water.

peaks to remaining water that may have contain free 4AT radicals. Therefore, EPR analysis shown in Fig. 15 proves that QD-4AT nanoprobes are homogeneously distributed on the polymer surface without any agglomeration. Binding of the QD-4AT nanoprobe to the polymer surface performed with the formation of amide bonds between the QD and the amine group on the polymer surface in the EDC/NHS reaction medium. The relevant mechanism is given in Sect. "QD attachment to functionalized thin films".

Fluorescence quenching mechanism

Tansakul et al. studied the examination of quenching efficiency by using different nitroxide radicals and reported that the nitroxide quenching efficiency depends on both the binding affinity and the proximity of the nitroxide moiety to the QD surface [12]. As a result of the study, it was seen that the proximity effect was dominant while the hydrogen bond also contributed to the quenching effect. The quenching efficiency is highly dependent on distance to QD surface; therefore, an electron exchange mechanism is more possible. This mechanism necessitates close proximity with the excited electron in the conduction band and should be favored for smaller nanoparticles [14]. Based on CdTe QDs used in this study (~ 2 to 3 nm), the electron exchange mechanism can be seen as the main mechanism for quenching, but more experiments are needed to evaluate the dependence of nitroxide fluorescence quenching on QD size.

To investigate fluorescence quenching of QD-4AT nanoprobes, fluorescence microscopy and spectroscopy analysis were performed. Fluorescence microscopy images of pGMA homopolymer films after QD and QD-4AT nanoprobe complex attachment process are shown in Fig. 16.

Fluorescence microscopy image shown in Fig. 16a shows pGMA homopolymer film after QD attachment procedure and the green emission of CdTe QDs indicates the QD attachment process was successful. On the other hand, Fig. 16b shows fluorescence microscopy image of pGMA film after QD-4AT nanoprobe complex attachment process. This image also indicates successful bonding of QD-4AT complex to polymer surface due to lack of typical green emission due to fluorescence quenching caused by 4AT. These observations agree well with the results of EPR analysis. Additionally, fluorescence spectroscopy analysis was performed using QD-4AT complex solution to investigate the effect of time on the fluorescence quenching. Fluorescence intensity vs wavelength plot of QD-4AT complex solution is shown in Fig. 17.

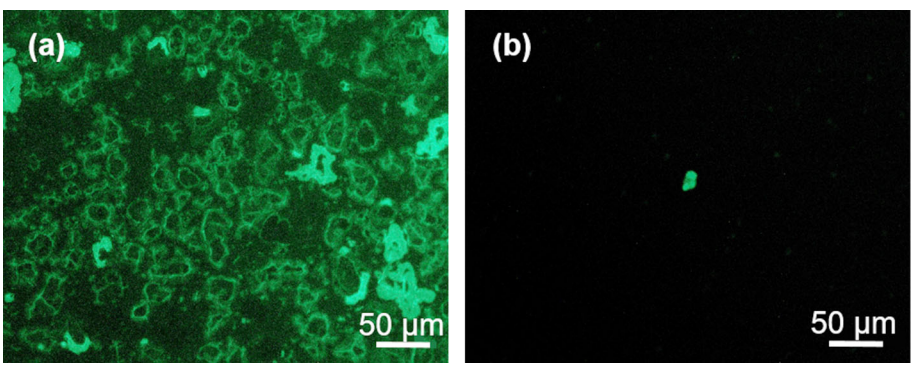

Figure 16 Fluorescence microscopy images of **a** CdTe QD attached pGMA homopolymer thin film surface and **b** QD-4AT attached pGMA homopolymer thin film surface.

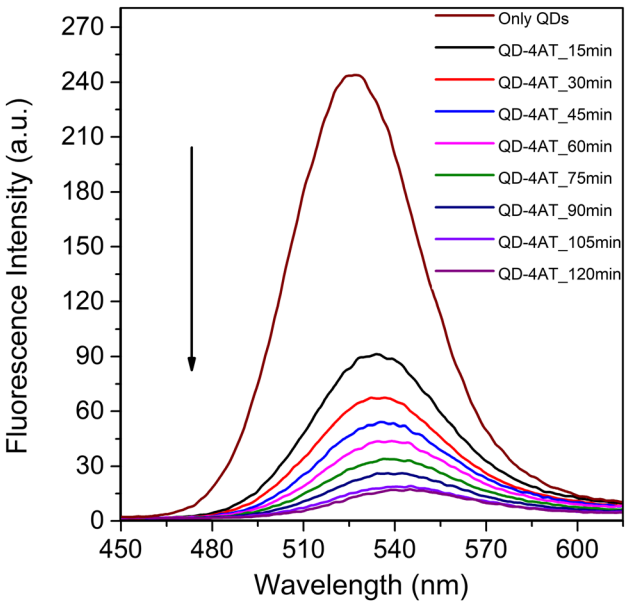

Figure 17 Fluorescence spectra of QD-4AT nanoprobe in water.

Figure 18 Visual inspection of QDs in water (left) and QD-4AT complex (right) approximately 24 h after preparation.

As expected, fluorescence spectra of QD-4AT complex solution shows a decrease in fluorescence intensity as more nitroxides bond to QD surface as time increases. Due to high 4AT concentration, the quenching rate was higher compared to similar studies in the literature [14, 84, 85]. It was observed that more than 50% quenching occurs in 15 min and after 120 min the fluorescence intensity does not decrease significantly. In addition, after formation of the QD-4AT complex, small red shift was observed compared with the only QDs fluorescence. This is related to surface modification of QD after interaction with 4AT and higher concentration of 4AT used for QD-4AT complex [14, 84, 85]. Fluorescence quenching can be also observed visually. The difference in fluorescence intensities between two samples one containing only CdTe QDs and other containing QD-4AT complex under UV light can be seen visually as shown in Fig. 18.

The significant decrease in fluorescence observed visually and confirmed by fluorescence spectroscopy shows the potential of using polymer bond QD-radical sensors as multiple-use, cheap and easy to use fluorescent sensors in various applications. The results obtained in this study indicate that the demonstrated polymer-bonded nanoprobe structure can be used for target material detection in fluorescence sensor studies.

Conclusion

A novel functional polymer-based QDs-nitroxide radical complex was demonstrated as nanoprobe for fluorescent sensors. The study was carried out in two parts: in the first part synthesis of pGMA and p(GMA-co-DEAEMA) copolymer thin films via iCVD method, amine group functionalization of these thin-films via epoxy ring opening reactions to achieve binding of CdTe QDs on the functionalized polymeric surfaces were demonstrated. Aromatic primary amine (aniline), aliphatic primary amine (propylamine) and aliphatic tertiary amine (Et_3N) were compared for nucleophilic epoxy ring opening reactions and QD attachment. Propylamine was found to be the most effective amine for functionalization of iCVD deposited pGMA and p(GMA-co-DEAEMA) thin-film surfaces and CdTe QD attachment to functionalized polymer surface.

In the second part of the study, the synthesis and attachment of QD-4AT nanoprobes to functionalized pGMA thin films and feasibility of using QD-4AT nanoprobes were investigated. In this part, study was carried out using only pGMA homopolymer since no significant difference was observed between pGMA and p(GMA-co-DEAEMA) polymers in terms of functionalization in the first part of the study. Characterization of QD-4AT nanoprobe was performed by EPR analysis by considering interaction time and

initial 4AT concentration. It was found that high initial 4AT concentration and longer (24 h) interaction time are beneficial as more nitroxide radicals bond to QD surface compared to 4 h interaction time. EPR analysis also revealed the existence of covalent bond between QD and 4AT when EDC was used during nanoprobe synthesis, and weak bonds when EDC was not used. In both cases, QD-4AT nanoprobes were successfully synthesized. Further EPR analysis together with fluorescence microscopy investigation confirmed successful attachment of QD-4AT nanoprobes to pGMA surface. The feasibility of using QD-4AT nanoprobes for fluorescent sensor applications based on fluorescence quenching was demonstrated by fluorescence microscopy and spectroscopy analysis. Time-depended fluorescence quenching analysis revealed that more than 50% reduction in fluorescence intensity, which can also be observed visually, occurred within 15 min demonstrating the possibility of using polymer bonded QD-4AT nanoprobes as multiple-use and easy to use as sensor structure in various applications.

Acknowledgements

This work was partially supported by the Scientific and Technological Research Council of Turkey (TUBITAK) (Grant Number 119M113). Authors would like to thank Prof. Dr. Yasar Akdogan for EPR analysis.

Author contributions

ÖE contributed to investigation, writing—review and editing, project administration, funding acquisition. MK contributed to conceptualization, investigation, methodology, formal analysis, writing—original draft, visualization.

Declarations

Conflict of interest The authors declare no competing financial interests.

References

[1] Wu J, Xia HG (2005) Tertiary amines as highly efficient catalysts in the ring-opening reactions of epoxides with amines or thiols in H2O: expeditious approach to β-amino alcohols and β-aminothioethers. Green Chem 7(10):708–710. https://doi.org/10.1039/B509288D

[2] Yu B, Lowe AB (2009) Synthesis of di- and tri-tertiary amine containing methacrylic monomers and their (co)polymerization via RAFT. J Polym Sci A Polym Chem 47(7):1877–1890. https://doi.org/10.1002/pola.23281

[3] Zhao X, Bagwe RP, Tan W (2004) Development of organic-dye-doped silica nanoparticles in a reverse microemulsion. Adv Mater 16(2):173–176. https://doi.org/10.1002/adma.200305622

[4] Serra PA (2011) New perspectives in biosensors technology and applications. IntechOpen.

[5] Liu Y, Teng L, Liu H-W, Xu C, Guo H, Yuan L, Zhang X-B, Tan W (2019) Recent advances in organic-dye-based photoacoustic probes for biosensing and bioimaging. Sci China Chem 62(10):1275–1285. https://doi.org/10.1007/s11426-019-9506-2

[6] Medintz IL, Uyeda TH, Goldman ER, Mattoussi H (2005) Quantum dot bioconjugates for imaging, labelling and sensing. Nat Mater 4(6):435–446. https://doi.org/10.1038/nmat1390

[7] Prabhakaran P, Kim WJ, Lee K-S, Prasad PN (2012) Quantum dots (QDs) for photonic applications. Opt Mater Expres 2(5):578–593. https://doi.org/10.1364/OME.2.000578

[8] Snee PT, Somers RC, Nair G, Zimmer JP, Bawendi MG, Nocera DG (2006) A ratiometric CdSe/ZnS nanocrystal pH sensor. J Am Chem Soc 128(41):13320–13321. https://doi.org/10.1021/ja0618999

[9] Selvan ST, Patra PK, Ang CY, Jackie YY (2007) Synthesis of silica-coated semiconductor and magnetic quantum dots and their use in the imaging of live cells. Angew Chem Int Ed 46(14):2448–2452. https://doi.org/10.1002/anie.200604245

[10] Liu W, Howarth M, Greytak AB, Zheng Y, Nocera DG, Ting AY, Bawendi MG (2008) Compact biocompatible quantum dots functionalized for cellular imaging. J Am Chem Soc 130(4):1274–1284. https://doi.org/10.1021/ja076069p

[11] Ünlütürk SS, Akdoğan Y, Özçelik S (2021) Mn^{2+} ions incorporated into ZnS x Se1−x colloidal quantum dots: controlling size and composition of nanoalloys and regulating magnetic dipolar interactions. Nanotechnology 32(16):165701. https://doi.org/10.1088/1361-6528/abdb65

[12] Tansakul C, Lilie E, Walter ED, Rivera F, Wolcott A, Zhang JZ, Millhauser GL, Braslau R (2010) Distance-dependent fluorescence quenching and binding of CdSe quantum dots by functionalized nitroxide radicals. J Phys Chem C 114(17):7793–7805. https://doi.org/10.1021/jp1005023

[13] Chen W, Wang X, Tu X, Pei D, Zhao Y, Guo X (2008) Water-soluble off–on spin-labeled quantum-dots conjugate. Small 4(6):759–764. https://doi.org/10.1002/smll.200700788

[14] Laferrière M, Galian RE, Maurela V, Scaiano JC (2006) Non-linear effects in the quenching of fluorescent quantum dots by nitroxyl free radicals. Chem Commun 3:257–259. https://doi.org/10.1039/B511515A

[15] Scaiano JC, Laferrière M, Galian RE, Maurel V, Billone P (2006) Non-linear effects in the quenching of fluorescent semiconductor nanoparticles by paramagnetic species. Phys Status Solidi A 203(6):1337–1343. https://doi.org/10.1002/pssa.200566186

[16] Adegoke O, Hosten E, McCleland C, Nyokonga T (2012) CdTe quantum dots functionalized with 4-amino-2,2,6,6-tetramethylpiperidine-N-oxide as luminescent nanoprobe for the sensitive recognition of bromide ion. Anal Chim Acta 721:154–161. https://doi.org/10.1016/j.aca.2012.01.040

[17] Xu K, Chen H, Wang H, Tian J, Li J, Li Q, Li N, Tang B (2011) A nanoprobe for nonprotein thiols based on assembling of QDs and 4-amino-2,2,6,6-tetramethylpiperidine oxide. Biosens Bioelectron 26(11):4632–4636. https://doi.org/10.1016/j.bios.2011.05.020

[18] Suvarapu LN, Baek SO (2015) Recent Developments in the speciation and determination of mercury using various analytical techniques. J Anal Methods Chem. https://doi.org/10.1155/2015/372459

[19] Fen YW, Yunus WMM (2013) Surface plasmon resonance spectroscopy as an alternative for sensing heavy metal ions: a review. Sens Rev 33(4):305–314. https://doi.org/10.1108/SR-01-2012-604

[20] Shen Y, Tingting LJH, Gao H, Hu Z (2019) Colorimetric and fluorogenic chemosensors for mercury ion based on nanomaterials. Prog Chem 31(4):536–549. https://doi.org/10.7536/PC180933

[21] Khanmohammadi A, Ghazizadeh AJ, Hashemi P, Afkhami A, Arduini F, Bagheri H (2020) An overview to electrochemical biosensors and sensors for the detection of environmental contaminants. J Iran Chem Soc 17(10):2429–2447. https://doi.org/10.1007/s13738-020-01940-z

[22] Li H, Wang X (2008) Single quantum dot-micelles coated with gemini surfactant for selective recognition of a cation and an anion in aqueous solutions. Sens Actuators B: Chem 134(1):238–244. https://doi.org/10.1016/j.snb.2008.04.041

[23] Koneswaran M, Narayanaswamy R (2009) RETRACTED: Mercaptoacetic acid capped CdS quantum dots as fluorescence single shot probe for mercury(II). Sens Actuators B: Chem 139(1):91–96. https://doi.org/10.1016/j.snb.2008.09.011

[24] De Acha N, Elosúa C, Corres JM, Arregui FJ (2019) Fluorescent sensors for the detection of heavy metal ions in aqueous media. Sensors 19(3):599. https://doi.org/10.3390/s19030599

[25] Dang YM, Guo XQ (2006) New approach for the detection of peptide- and protein-based radicals using a pre-fluorescent probe. Appl Spectrosc 60(2):203–207

[26] Lin F, Pei D, He W, Huang Z, Huanga Y, Guo X (2012) Electron transfer quenching by nitroxide radicals of the fluorescence of carbon dots. J Mater Chem 22(23):11801–11807. https://doi.org/10.1039/C2JM31191G

[27] Bian ZY, Guo XQ, Zhao YB, Du JO (2005) Probing the hydroxyl radical-mediated reactivity of peroxynitrite by a spin-labeling fluorophore. Anal Sci Int J Jpn Soc Anal Chem 21(5):553–559. https://doi.org/10.2116/analsci.21.553

[28] Green SA, Simpson DJ, Zhou G, Ho PS, Blough NV (1990) Intramolecular quenching of excited singlet states by stable nitroxyl radicals. J Am Chem Soc 112(20):7337–7346. https://doi.org/10.1021/ja00176a038

[29] Maurel V, Laferrière M, Billone P, Godin R, Scaiano JC (2006) Free radical sensor based on CdSe quantum dots with added 4-amino-2,2,6,6-tetramethylpiperidine oxide functionality. J Phys Chem B 110(33):16353–16358. https://doi.org/10.1021/jp061115d

[30] Zhou T, Zhua Y, Lia X et al (2016) Surface functionalization of biomaterials by radical polymerization. Prog Mater Sci 83:191–235. https://doi.org/10.1016/j.pmatsci.2016.04.005

[31] McElroy N, Page RC, Espinbarro-Valazquez D, Lewis E, Haigh S, Brien PO, Binks DJ (2014) Comparison of solar cells sensitised by CdTe/CdSe and CdSe/CdTe core/shell colloidal quantum dots with and without a CdS outer layer. Thin Solid Films 560:65–70. https://doi.org/10.1016/j.tsf.2013.10.085

[32] Xu JJ, Gleason KK (2010) Conformal, amine-functionalized thin films by initiated chemical vapor deposition (iCVD) for hydrolytically stable microfluidic devices. Chem Mater 22(5):1732–1738. https://doi.org/10.1021/cm903156a

[33] Özpirin M, Ebil Ö (2018) Transparent block copolymer thin films for protection of optical elements via chemical vapor deposition. Thin Solid Films 660:391–398. https://doi.org/10.1016/j.tsf.2018.06.044

[34] Hoffman AS (1996) Surface modification of polymers: Physical, chemical, mechanical and biological methods. Macromol Symp 101(1):443–454. https://doi.org/10.1002/masy.19961010150

[35] Nemani SK, Annavarapu RK, Mohammadian B, Raiyan A, Heil J, Haque MA, Abdelaal A, Sojoudi H (2018) Surface modification of polymers: methods and applications. Adv Mater Interfaces 5(24):1801247. https://doi.org/10.1002/admi.201801247

[36] Pinson J, Thiry D (2019) Surface modification of polymers: methods and applications, 1st edn. Wiley
[37] Shimpi NG (2017) Biodegradable and biocompatible polymer composites: processing, properties and applications, 1st edn. Elsevier Science
[38] Mittal KL (2009) Polymer surface modification: relevance to adhesion, 1st edn. Taylor & Francis
[39] Asatekin A, Barr MC, Baxamusa SH, Lau KKS, Tenhaeff W, Xu J, Gleason KK (2010) Designing polymer surfaces via vapor deposition. Mater 13(5):26–33. https://doi.org/10.1016/S1369-7021(10)70081-X
[40] Jaganathan SK, Balaji A, Vellayappan MV, Subramanian AP, John AA, Asokan MK, Supriyanto E (2015) Review: radiation-induced surface modification of polymers for biomaterial application. J Mater Sci 50(5):2007–2018. https://doi.org/10.1007/s10853-014-8718-x
[41] Sarıipek F, Karaman M (2014) Initiated CVD of tertiary amine-containing glycidyl methacrylate copolymer thin films for low temperature aqueous chemical functionalization. Chem Vap Depos. https://doi.org/10.1002/cvde.201407129
[42] Li G, Zhu XL, Zhu J, Cheng ZP, Zhang W (2005) Homogeneous reverse atom transfer radical polymerization of glycidyl methacrylate and ring-opening reaction of the pendant oxirane ring. Polymer 46(26):12716–12721. https://doi.org/10.1016/j.polymer.2005.10.061
[43] Gleason KK (2015) CVD polymers: fabrication of organic surfaces and devices, 1st edn. Wiley
[44] Coclite AM, Ozaydin-Ince G, d'Agostino R, Gleason KK (2009) Flexible cross-linked organosilicon thin films by initiated chemical vapor deposition. Macromolecules 42(21):8138–8145. https://doi.org/10.1021/ma901431m
[45] Aresta G, Palmans J (2012) Initiated-chemical vapor deposition of organosilicon layers: monomer adsorption, bulk growth, and process window definition. J Vac Sci Tachnol. https://doi.org/10.1116/1.4711762
[46] Lau KKS, Bico J, Teo KB, Chhowalla M, Amaratunga GAJ, Milne WI, McKinley GH, Gleason KK (2003) Superhydrophobic carbon nanotube forests. Nano Lett 3(12):1701–1705. https://doi.org/10.1021/nl034704t
[47] Lau KKS, Gleason KK (2006) Initiated chemical vapor deposition (iCVD) of poly(alkyl acrylates): a kinetic model. Macromolecules 39(10):3695–3703. https://doi.org/10.1021/ma0601621
[48] Lau KKS, Gleason KK (2006) Initiated chemical vapor deposition (iCVD) of poly(alkyl acrylates): an experimental study. Macromolecules 39(10):3688–3694. https://doi.org/10.1021/ma0601619
[49] Lau KKS, Gleason KK (2007) All-dry synthesis and coating of methacrylic acid copolymers for controlled release. Macromol Biosci 7(4):429–434. https://doi.org/10.1002/mabi.200700017
[50] Lau KKS, Gleason KK (2007) Particle functionalization and encapsulation by initiated chemical vapor deposition (iCVD). Surf Coat Technol 201(22–23):9189–9194. https://doi.org/10.1016/j.surfcoat.2007.04.045
[51] Lee W, Oshikiri T, Saito K, Sugita K, Sugo T (1996) Comparison of formation site of graft chain between nonporous and porous films prepared by RIGP. Chem Mater 8(11):2618–2621. https://doi.org/10.1021/cm950405w
[52] Labbé A, Brocas AL, Ibarboure E, Ishizone T, Hirao A, Deffieux A, Carlotti S (2011) Selective ring-opening polymerization of glycidyl methacrylate: toward the synthesis of cross-linked (Co) polyethers with thermoresponsive properties. Macromolecules 44(16):6356–6364. https://doi.org/10.1021/ma201075n
[53] Muzammil EM, Khan A, Stuparu MC (2017) Post-polymerization modification reactions of poly(glycidyl methacrylate)s. RSC Adv 7(88):55874–55884. https://doi.org/10.1039/C7RA11093F
[54] Zhang MQ, Rong MZ (2011) Self-healing polymers and polymer composites, 1st edn. Wiley
[55] Kim M, KiyoharaS KS, Tsuneda S, Saito K, Sugod T (1996) Ring-opening reaction of poly-GMA chain grafted onto a porous membrane. J Membr Sci 117(1):33–38. https://doi.org/10.1016/0376-7388(96)00026-9
[56] Lau KKS, Gleason KK (2006) Particle surface design using an all-dry encapsulation method. Adv Mater 18(15):1972–1977. https://doi.org/10.1002/adma.200600896
[57] Tarducci C, Kinmond EJ, Badyal JPS, Brewer SA, Willis C (2000) Epoxide-functionalized solid surfaces. Chem Mater 12(7):1884–1889. https://doi.org/10.1021/cm0000954
[58] Allcock HR, Nelson CJ, Coggio WD (1994) Photoinitiated graft poly(organophosphazenes): functionalized immobilization substrates for the binding of amines. Proteins Metals Chem Mater 6(4):516–524. https://doi.org/10.1021/cm00040a029
[59] Zhang J, Ikada Y, Kato K (1995) Surface graft polymerization of glycidyl methacrylate onto polyethylene and the adhesion with epoxy resin. J Polym Sci Part A: Polym Chem 33(15):2629–2638. https://doi.org/10.1002/pola.1995.080331509
[60] Allmér K, Hult A, Rånby B (1989) Surface modification of polymers. II. Grafting with glycidyl acrylates and the reactions of the grafted surfaces with amines. J Polym Sci Part A: Polym Chem 27(5):1641–1652. https://doi.org/10.1002/pola.1989.080270516
[61] Mori M, Uyama Y, Ikada Y (1994) Surface modification of polyethylene fiber by graft polymerization. J Polym Sci A

Polym Chem 32(9):1683–1690. https://doi.org/10.1002/pola.1994.080320910

[62] Kimmins SD, Wyman P, Cameron NR (2014) Amine-functionalization of glycidyl methacrylate-containing emulsion-templated porous polymers and immobilization of proteinase K for biocatalysis. Polymer 55(1):416–425. https://doi.org/10.1016/j.polymer.2013.09.019

[63] Baxamusa SH, Im SG, Gleason KK (2009) Initiated and oxidative chemical vapor deposition: a scalable method for conformal and functional polymer films on real substrates. Phys Chem 11(26):5227–5240. https://doi.org/10.1039/B900455F

[64] Alf ME, Asatekin A, Barr MC et al (2010) Chemical vapor deposition of conformal, functional, and responsive polymer films. Adv Mater 22(18):1993–2027. https://doi.org/10.1002/adma.200902765

[65] Barbey R, Klok HA (2010) Room temperature, aqueous post-polymerization modification of glycidyl methacrylate-containing polymer brushes prepared via surface-initiated atom transfer radical polymerization. Langmuir 26(23):18219–18230. https://doi.org/10.1021/la102400z

[66] Drzal TL (1986) Advances in Polymer Science-Epoxy Resins and Composites II.

[67] Lee AN, Kennedy IR (2007) Chapter 5 - Immunoassays. Food Toxicants Analysis. Elsevier, Amsterdam, pp 91–145

[68] Rizvi S, Sebideh R, Taniguchi S, Yang SY, Green M, Keshtgar M, Seifalian A (2014) Near-infrared quantum dots for HER2 localization and imaging of cancer cells. Int J Nanomed 9(1):1323–1337. https://doi.org/10.2147/IJN.S51535

[69] Shen L (2011) Biocompatible polymer/quantum dots hybrid materials: current status and future developments. J Funct Biomater 2(4):355–372. https://doi.org/10.3390/jfb2040355

[70] Gunzler H, Gremlich HU (2002) IR Spectroscopy. Wiley-VCH

[71] Safiullah MS, Abdul WK, Anver BK (2014) Preparation of poly(Glycidyl methacrylate)–copper nanocomposite by in-situ suspension polymerization—A novel synthetic method. Mater Lett 133:60–63. https://doi.org/10.1016/j.matlet.2014.06.127

[72] Bakker R, Verlaan V, van der Werf CHM, Rath JK, Gleason KK, Schropp REI (2007) Initiated chemical vapour deposition (iCVD) of thermally stable poly-glycidyl methacrylate. Surf Coat Tech 201(22–23):9422–9425. https://doi.org/10.1016/j.surfcoat.2007.03.058

[73] Karaman M, Çabuk N (2012) Initiated chemical vapor deposition of pH responsive poly(2-diisopropylamino)ethyl methacrylate thin films. Thin Solid Films 520(21):6484–6488. https://doi.org/10.1016/j.tsf.2012.06.083

[74] Mao Y, Gleason KK (2006) Vapor-deposited fluorinated glycidyl copolymer thin films with low surface energy and improved mechanical properties. Macromolecules 39(11):3895–3900. https://doi.org/10.1021/ma052591p

[75] Mao Y, Gleason KK (2004) Hot filament chemical vapor deposition of poly(glycidyl methacrylate) thin films using tert-butyl peroxide as an initiator. Langmuir 20(6):2484–2488. https://doi.org/10.1021/la0359427

[76] Bayramoglu G, Bitirim VC, Tunalı Y, Arica MY, Akcali K (2013) Poly (hydroxyethyl methacrylate-glycidyl methacrylate) films modified with different functional groups: in vitro interactions with platelets and rat stem cells. Mater Sci Eng C 33(2):801–810. https://doi.org/10.1016/j.msec.2012.11.004

[77] d'Ischia M, Ruiz-Molina D (2018) Bioinspired catechol-based systems: chemistry and applications MDPI AG. Biomimetics. https://doi.org/10.3390/biomimetics2040025

[78] Shanmugharaj AM, Yoon JH, Yang WJ, Ryu SH (2013) Synthesis, characterization, and surface wettability properties of amine functionalized graphene oxide films with varying amine chain lengths. J Colloid Interface Sci 401:148–154. https://doi.org/10.1016/j.jcis.2013.02.054

[79] Enikolopiyan NS (1976) New aspects of the nucleophilic opening of epoxide rings. Pure Appl Chem 48(3):317–328. https://doi.org/10.1351/pac197648030317

[80] Schreier S, Ernandes RJ, Cuccovia I, Chaimovich H (1978) Spin label studies of structural and dynamical properties of detergent aggregates. J Magn Reson 30(2):283–298. https://doi.org/10.1016/0022-2364(78)90102-6

[81] Blaskó Á, Gazdag Z, Grof P, Mate G (2017) Effects of clary sage oil and its main components, linalool and linalyl acetate, on the plasma membrane of Candida albicans: an in vivo EPR study. Apoptosis 22(2):175–187. https://doi.org/10.1007/s10495-016-1321-7

[82] Yildiz R, Özen S, Şahin H, Akdoğan Y (2020) The effect of DOPA hydroxyl groups on wet adhesion to polystyrene surface: an experimental and theoretical study. Mater Chem Phys 243:122606. https://doi.org/10.1016/j.matchemphys.2019.122606

[83] Göksel Y, Akdogan Y (2019) Increasing spontaneous wet adhesion of DOPA with gelation characterized by EPR spectroscopy. Mater Chem Phys 228:124–130. https://doi.org/10.1016/j.matchemphys.2019.02.054

[84] Jin WJ, Fernández CJM, Pereiro R, Medel AS (2004) Surface-modified CdSe quantum dots as luminescent probes for

cyanide determination. Anal Chim Acta 522:1–8. https://doi.org/10.1016/j.aca.2004.06.057

[85] Diaz D, Robles J, Ni T, Castillo-Blum S, Nagesha D, Alvarez-Fregoso OJ, Kotov NA (1999) Surface modification of CdS Nanoparticles with MoS42-: a case study of nanoparticle−modifier electronic interaction. J Phys Chem B 103(45):9859–9866. https://doi.org/10.1021/jp992122n